

졸업논문청구논문

**단결정 페로브 스카이트의 PL측정을 통한
exciton과 biexciton peak의 분석**

**Analysis of exciton and biexciton peaks by PL
measurement of single crystal perovskite**

김 주 원 (李 善 在 Lee, Seon Jae)

16072

과학영재학교 경기과학고등학교

2019

단결정 폐로브 스카이트의 PL측정을 통한 exciton과 biexciton peak의 분석

**Analysis of exciton and biexciton peaks by PL
measurement of single crystal perovskite**

[논문제출 전 체크리스트]

1. 이 논문은 내가 직접 연구하고 작성한 것이다.
2. 인용한 모든 자료(책, 논문, 인터넷자료 등)의 인용표시를 바르게 하였다.
3. 인용한 자료의 표현이나 내용을 왜곡하지 않았다.
4. 정확한 출처제시 없이 다른 사람의 글이나 아이디어를 가져오지 않았다.
5. 논문 작성 중 도표나 데이터를 조작(위조 혹은 변조)하지 않았다.
6. 다른 친구와 같은 내용의 논문을 제출하지 않았다.

Analysis of exciton and biexciton peaks by PL measurement of single crystal perovskite

Advisor : Teacher Park, Kie Hyun

by

16072 Lee, Seon Jae

Gyeonggi Science High School for the gifted

A thesis submitted to the Gyeonggi Science High School in partial fulfillment of the requirements for the graduation. The study was conducted in accordance with Code of Research Ethics.*

2018. 7. 21.

Approved by
Teacher Park, Kie Hyun
[Thesis Advisor]

*Declaration of Ethical Conduct in Research: I, as a graduate student of GSHS, hereby declare that I have not committed any acts that may damage the credibility of my research. These include, but are not limited to: falsification, thesis written by someone else, distortion of research findings or plagiarism. I affirm that my thesis contains honest conclusions based on my own careful research under the guidance of my thesis advisor.

단결정 폐로브 스카이트의 PL측정을 통한 exciton과 biexciton peak의 분석

김 주 원

위 논문은 과학영재학교 경기과학고등학교 졸업논문으로
졸업논문심사위원회에서 심사 통과하였음.

2018년 7월 21일

심사위원장 박 용 선 (인)

심사위원 강 동 일 (인)

심사위원 박 기 현 (인)

Analysis of exciton and biexciton peaks by PL measurement of single crystal perovskite

Abstract

Stars are born when matter from interstellar molecular clouds fall to the center to increase the mass of the protostar. Bipolar outflows are formed to remove the excess angular momentum of falling matter. Intensities of outflows are known to be in a close relationship with their bolometric luminosity and evolutionary stages. In this study, data from Institute for Radio Astronomy in the Millimeter Range (IRAM) 30m Telescope and Taeduk Radio Astronomy Observatory (TRAO) were used. IRAM data were used to map ^{12}CO $J = 2 - 1$ over Orion A molecular cloud. TRAO data were used to map ^{13}CO $J = 1 - 0$ over the same region. Outflows were observed and measured by drawing contour maps and line profiles of red/blue shifted components. The correlation between a protostar's luminosity and outflow momentum flux have been confirmed. Also, outflows could be detected better if the energy level of the emission line is higher.

단결정 페로브 스카이트의 PL측정을 통한 exciton과 biexciton peak의 분석

초 록

별은 성간분자운의 물질이 중심으로 떨어져 원시성의 질량을 증가시켜야만 탄생된다. 이 과정에서 중심으로 떨어지는 물질의 각운동량을 제거하기 위해 방출류가 발생한다. 여기서 방출류의 세기는 원시성의 진화 단계와 광도와 관련이 있다고 알려져 있다. 이를 새로 관측된 데이터를 사용하여 기존의 연구를 검증해 보려고 한다. 이 연구에서는 Institute for Radio Astronomy in the Millimeter Range (IRAM) 30m 망원경으로 관측한 ^{12}CO $J = 2 - 1$ 관측 자료와 대덕 전파 망원경(Taeduk Radio Astronomy Observatory, TRAO)으로 관측한 ^{13}CO $J = 1 - 0$ 천이 선 자료를 이용하였다. 두 자료 모두 Orion A Cloud 영역을 담고 있다. 빠른 속도를 가진 적색/청색편이된 성분의 contour map을 그려 방출류를 관찰하고 방출류의 세기를 구하였다. 방출류의 세기와 원시성의 광도가 대체적으로 비례한다는 것을 알 수 있었다. 그리고 천이 선의 에너지 준위가 높을수록 방출류를 더 잘 검출할 수 있음을 확인할 수 있었다.

Contents

Abstract	i
Contents	iii
List of Figures	iv
List of Tables	v
I 서론	1
I.1 연구 동기	1
I.2 이론적 배경	1
I.2.1 Perovskite	1
I.2.2 PL	2
I.2.3 선행연구 및 한계	2
II Observations and Data Reduction	3
II.1 Observation Region	3
II.2 Observation Data	3
II.3 Identification of Outflows	4
II.4 Calculating Momentum Flux	6
III Results	7
III.1 Outflow Identification	7
III.1.1 ^{12}CO $J = 2 - 1$ Observations	8
III.1.2 ^{12}CO $J = 1 - 0$ Observations	12
III.2 Momentum Flux	13
III.3 Momentum flux vs. Bolometric luminosity	14
III.4 Momentum flux by emission line energy level	15

IV Conclusion	16
연구활동	17

List of Figures

Figure 1.	Orion A ^{12}CO ($J = 2 - 1$) integrated intensity map (left) ^{13}CO ($J = 1 - 0$) integrated intensity map (right).	4
Figure 2.	The ^{12}CO $J = 2 - 1$ intensity contour map (left) and the line profile (right) of FIR2.	8
Figure 3.	The contour map and the line profile of FIR3.	8
Figure 4.	The contour map and the line profile of FIR6b.	9
Figure 5.	The contour map and the line profile of MMS2.	9
Figure 6.	The contour map and the line profile of MMS5.	10
Figure 7.	The contour map and the line profile of MMS9.	10
Figure 8.	The ^{12}CO $J = 1 - 0$ intensity contour map of FIR2 (left), FIR3 (middle), and MMS9 (right).	12
Figure 9.	CO outflow momentum flux vs. L_{bol}	14
Figure 10.	Momentum flux difference by emission line energy.	15

List of Tables

Table 1.	Protostars with observed outflows.	7
Table 2.	CO outflow parameters.	13

I. 서론

I.1 연구 동기

Perovskite 구조를 가지고 있는 결정에 레이저를 쏘았을 때 빛이 결정의 바깥쪽으로 퍼지는 현상을 관찰할 수 있었고, wave guiding effect에 의한 현상으로 판단하였다. 기존의 perovskite의 구조, 광학적 특성을 분석한 실험에서는 XRD, TRPL, PL등 여러가지 장비를 통해 분석을 하였지만 각각의 장비에 대해서는 깊게 분석하지 못한 면들이 있었다. 특히 PL 분석에서는 PL로 찍었을 때 나오는 개형의 half width과 peak에 대해서만 분석하였기에 exciton peak과 biexciton peak에 대해서 따로 분석해보고자 하였다.

I.2 이론적 배경

I.2.1 Perovskite

Perovskite는 L. A. Perovski의 이름을 따서 명명된 물질로, 처음 발견된 CaTiO₃ 같은 구조를 가진 결정을 통틀어서 부르는 말이다. 일반적으로 ABX₃로 쓰며, A와 M에는 여러 금속 양이온들이 해당되고, X에는 보통 16족, 17족 음이온들이 해당된다. A위치에는 금속뿐만 아니라 유기물인 methylammonium (CH_3NH_3^+)이나 ethylammonium ($\text{CH}_3\text{CH}_2\text{NH}_3^+$)를 넣어 폐로브스카이트를 구성할 수 있다. 쇼트키-퀘이서 효율 한계(Shockley Queisser Efficiency Limit)에 의하면 물질의 밴드갭에 따라 전지 효율의 이론적 최댓값이 존재한다. 폐로브스카이트는 각 자리에 여러 물질을 바꿔 넣을 수 있으므로 이론적인 최대 효율값에 비슷하게 도달할 수 있는 장점이 있다. 이 뿐만 아니라 가능한 밴드갭 영역이 넓고 꼭짓점을 공유하는 팔면체들의 희로망 덕분에 캐리어의 이동성이 좋아서 전하가 잘 수송되기도 한다.[4] 또, 폐로브스카이트는 합성이 간편하며 태양빛을 잘 흡수하기 때문에 각광받고 있으며, 이와 관련되어 여러 연구가 진행되고 있다. 최근 연구에서는 폐로브스카이트에 defect가 존재하여 물성을 탐색할 때 정확하지 못하다는 문제를 해결하기 위해서 단결정을 제작하기도

한다. 본 연구에서는 단결정을 제작하는 새로운 방식 중 하나인 PDMS stamping을 이용하여 단결정을 제작하였다.

I.2.2 PL

PL(Photoluminescence)는 광자를 통해 에너지를 흡수한 물질이 그 에너지를 다시 방출하는 것을 이르는 것이다. 이론적으로는 넣어준 빛의 파장과 동일한 파장의 빛이 나올 수도 있지만 보통은 에너지가 더 낮은, 파장이 더 긴 빛이 방출되게 된다. 위 그림에서처럼 빛이 방출되는 과정은 크게 세 가지로 나뉘는데, photoexcitation, relaxation, radiative recombination 과정으로 나뉜다. photoexcitation은 외부에서 주어진 빛에 의해 전자가 들뜨는 현상을 이르는 것이고 relaxation은 들뜬 전자가 전도띠에서 에너지가 가장 낮은 부분으로, 정공이 원자띠에서 에너지가 가장 높은 부분으로 오는 과정이다. 마지막으로 radiative recombination 과정은 들뜬 전자가 다시 정공과 결합하는 과정을 의미한다. 이때 방출되는 빛을 이용하여 물질의 밴드갭을 알 수 있다.

I.2.3 선행연구 및 한계

이전에 했던 단결정 폐로브 스카이트의 구조적 광학적 특성 분석에 관한 연구에서 XRD와 TRPL, PL을 통하여서 구조적, 광학적 특성을 분석하였다. XRD는 성공적이었으나 위치별로 분석한 PL 분석에서는 스펙트럼이 비대칭적으로 나타났음에도 불구하고 peak와 half width로만 분석했기에 경향성을 분석할 때에 exciton peak 와 biexciton peak의 합의 경향성을 볼 수 있었다. 반면에 exciton 과 biexciton 에 대한 경향성을 따로 볼 수 없었다는 것에 한계가 있다.

II. Observations and Data Reduction

II.1 Observation Region

The Orion region consists of two giant molecular clouds, the Orion A and B clouds. This study covers the Orion A Cloud. The Orion A Cloud covers about 29 deg^2 of the sky and its distance is about 450pc [?]. The total mass is estimated to be about $10^5 M_\odot$. It contains several hot molecular cores, such as the BN-KL nebula. It is known that the Orion Cloud was formed by the collision and fragmentation of two giant molecular clouds about 60 million years ago. The effects of the collision can be seen in the present. There is a big velocity gradient along the declination axis. The north side of the Orion A Cloud (OMC 2) shows about 12 km s^{-1} but the south end (L1641) it is about 5 km s^{-1} [?].

II.2 Observation Data

The ^{12}CO ($J = 2 - 1$, 230.538 GHz) data was observed with the IRAM 30 m telescope in Granada, Spain, in 2013. The spatial beamwidth was $11''$, and the spectral resolution was 0.4 km s^{-1} . The noise level was 0.2K. It only covers the north region of the Orion A cloud [?].

The ^{12}CO ($J = 1 - 0$, 115.271 GHz) data was observed with the NRO 45m telescope in Nobeyama, Japan.

The ^{13}CO ($J = 1 - 0$, 110.201 GHz) and the C^{18}O ($J = 1 - 0$, 109.782 GHz) data were observed with the 13.7 m telescope at Taeduk Radio Astronomy Observatory (TRAO) in 2017. The spatial beamwidth was $45''$, and the spectral resolution was 0.05 km s^{-1} . The noise level was 0.4K. ^{13}CO and C^{18}O lines are optically thin lines which can trace most of the matter on the line of sight, contrasting to ^{12}CO lines which are so optically opaque that it can only trace the outermost part of the molecular core. In this study, I used TRAO data to determine the

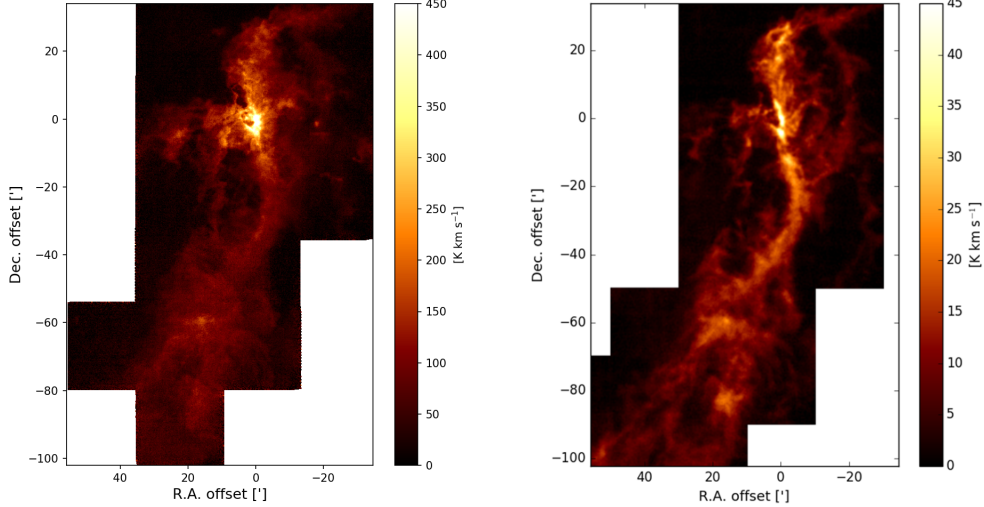


Figure 1. Orion A ^{12}CO ($J = 2 - 1$) integrated intensity map (left) ^{13}CO ($J = 1 - 0$) integrated intensity map (right).

protostar's velocity and linewidth which are the kinematic properties of the envelope. Then, I traced the outflow jets using ^{12}CO data.

Figure 1 shows the data from IRAM and TRAO. The intensity of the ^{12}CO data is approximately 10 times stronger than the ^{13}CO data.

II.3 Identification of Outflows

Data obtained by observing radio waves were summed over the line of sight, which tells us the distribution of matter with a relative radial velocity to the observer. The envelope around the protostar is static or is contracting slowly towards the protostar itself, but the outflow jets have large velocity components from each pole. If the inclination of the outflows are not zero, it would appear like the jets are moving closer to or further from the observer. In this study, ^{13}CO and C^{18}O lines were used to get the velocity distribution of the protostar. By using Gaussian fitting to the velocity distribution, I calculated the protostar's central velocity(v_{cen}) and the full

width at half maximum (FWHM).

Because the emission lines of ^{12}CO are optically thicker than other lines, it is appropriate to trace the outflows with ^{12}CO lines. The intervals of the red/blue lobes were obtained by using the central velocity and the FWHM calculated previously. I drew contour maps to find out if bipolar outflows existed with the protostar at the center. To check if the red/blue lobes that were found are outflows from the same protostar I checked the ^{12}CO , ^{13}CO , C^{18}O lines from the red peak, blue peak, and the center points. For each outflow confirmed, I calculated the momentum force and the column density of each point.

The column density can be calculated with the following expression:

$$N_{\text{H}_2} = \frac{8\pi v^3}{c^3} \frac{1}{(2J_l + 3)A} \times \frac{Z(T_{ex})}{\exp(-E_l/kT_{ex})[1 - \exp(hv/kT_{ex})]} \times \frac{\int T_B dV}{J(T_{ex}) - J(T_{bg})} \quad (1)$$

$$J(T) = \frac{hv/k}{\exp(hv/kT) - 1} \quad (2)$$

In equation (1), v is the corresponding frequency of the emission line, c is the speed of light, J_l is the rotational quantum number of the lower energy level, A is the Einstein A coefficient, Z is the partition function, E_l is the rotational energy of the lower energy level, k is the Boltzmann's constant, T_{ex} is the excitation temperature of the transitions, $\int T_B dV$ is the integrated intensity measured, and T_{bg} is the background radiation temperature. I assumed a local thermal equilibrium(LTE) excitation at an outflow temperature of 50K [?]. The mass within one beam can be calculated as the following:

$$M_B = \frac{\pi}{4} D^2 \theta_B^2 X[\text{CO}] N_{\text{H}_2} m_{\text{H}_2} \quad (3)$$

D is the distance to the objects, θ_B is the beam size, and m_{H_2} is the mass of one hydrogen molecule. $X[\text{CO}]$ is the abundance ratio of CO to H₂. In this paper, $D = 450\text{pc}$ and $X[\text{CO}] = 10^{-4}$ was used [?].

II.4 Calculating Momentum Flux

The momentum flux within one beam is calculated with the following:

$$\dot{P} = \frac{dP}{dt} = \sum_v \frac{M_B(v)(v/\cos i)}{D\theta_B/(v\tan i)} \quad (4)$$

v is the velocity offset from v_{cen} , $M_B(v)$ is the mass within one beam, and i is the inclination within one beam [?]. Then the momentum flux from individual beams were summed in annuli.

$$F_{\text{CO}} = \sum_{\text{annulus}} \frac{2\pi\theta_r}{N_{\text{pix}}\theta_B} \dot{P} \quad (5)$$

N_{pix} is the number of pixels in an annulus. θ_r is the distance between each pixel and the outflow center. θ_B is the beam size [?, ?].

III. Results

III.1 Outflow Identification

Table 1. Protostars with observed outflows.

Name	Coordinates		L_{bol} [L_\odot]	T_{bol} [K]
	RA	Dec		
FIR2	05:35:24.3	-05:08:33.3	5.68	100.6
FIR3	05:35:27.5	-05:09:32.5	360.86	71.5
FIR6b	05:35:23.4	-05:12:03.2	21.93	54.1
MMS2	05:35:18.3	-05:00:34.8	20.11	186.3
MMS5	05:35:22.4	-05:01:14.1	15.81	42.4
MMS9	05:35:26.0	-05:05:42.4	8.91	38.1

Table 1 shows the protostars with bipolar outflows observed. The names of the protostars are from the 1.3mm continuum observations by Chini et al. [?] and Nielbock et al. [?] L_{bol} and T_{bol} were calculated from the Spitzer and Herschel surveys [?, ?].

III.1.1 ^{12}CO $J = 2 - 1$ Observations

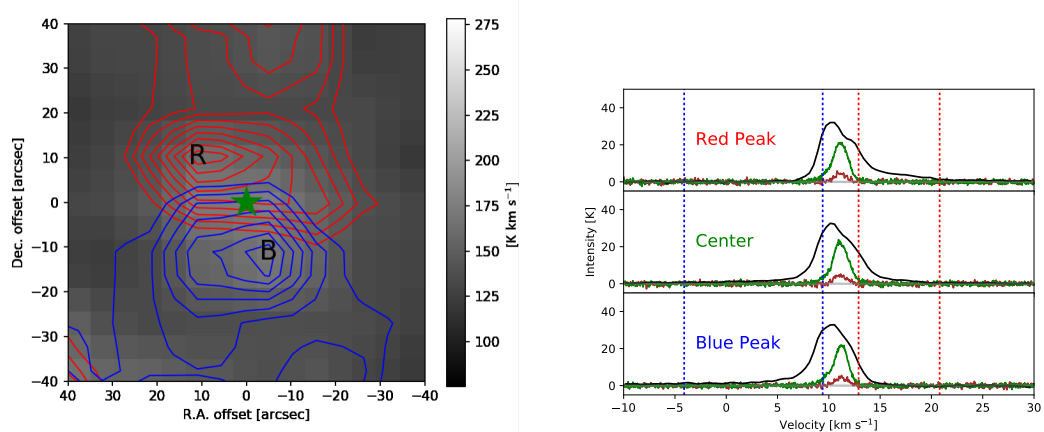


Figure 2. The ^{12}CO $J = 2 - 1$ intensity contour map (left) and the line profile (right) of FIR2.

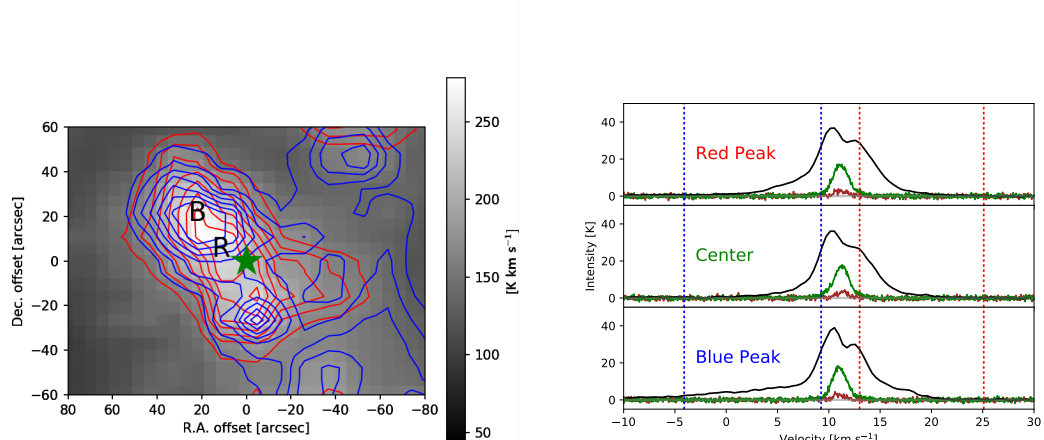


Figure 3. The contour map and the line profile of FIR3.

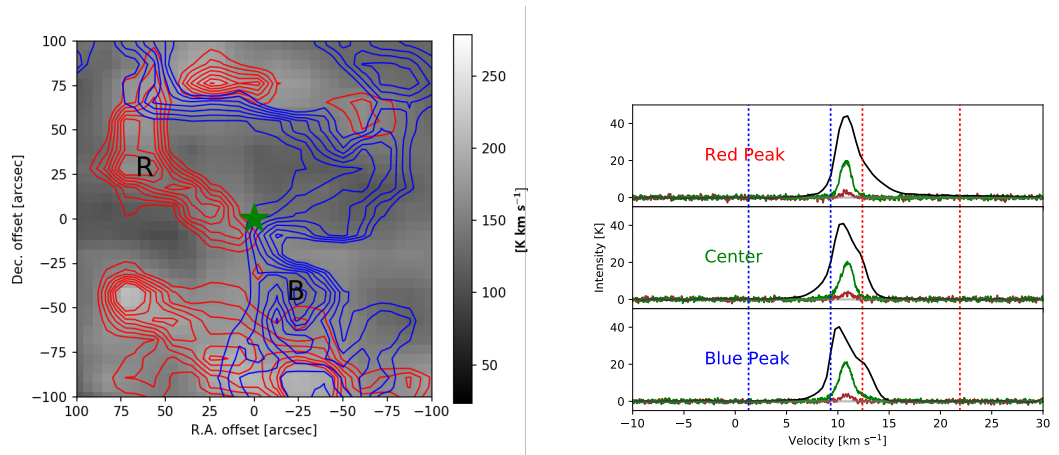


Figure 4. The contour map and the line profile of FIR6b.

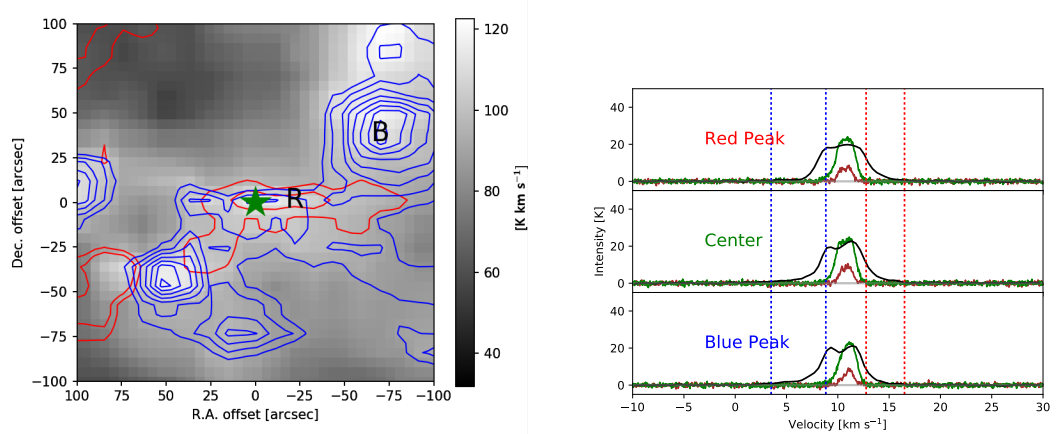


Figure 5. The contour map and the line profile of MMS2.

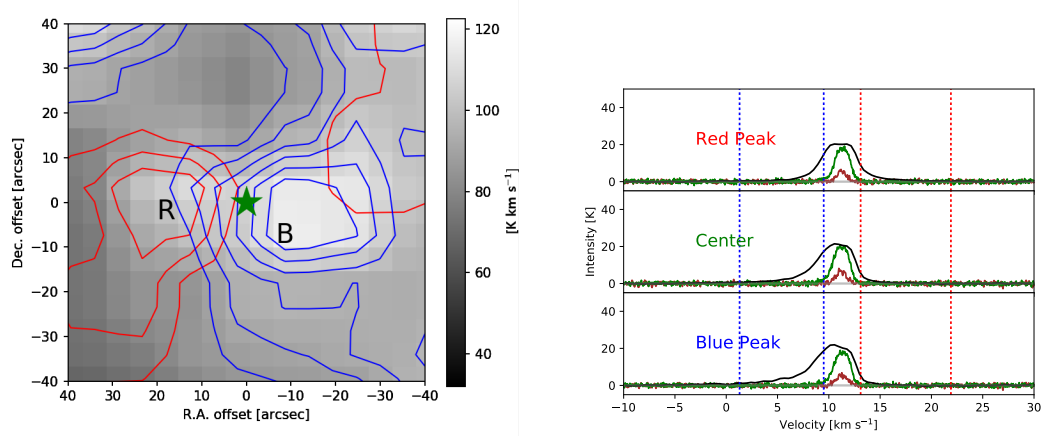


Figure 6. The contour map and the line profile of MMS5.

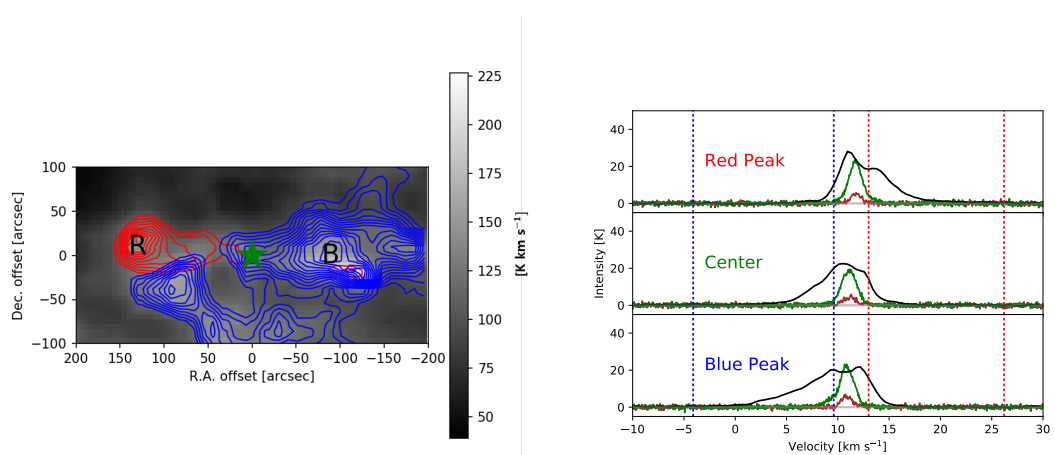


Figure 7. The contour map and the line profile of MMS9.

The ^{12}CO $J = 2 - 1$ intensity for each point were calculated by using equations (1) and (3). The line profile shows the intensities of ^{12}CO $J = 2 - 1$ (black), ^{13}CO $J = 1 - 0$ (green), and C^{18}O $J = 1 - 0$ (brown) for each point.

FIR2 – There is a strong bipolar outflow elongated along the N-S direction as shown in Figure 2. The size is about 30 arcsec, which is smaller than other outflows detected. Red and blue contour intervals are 10σ starting from 60σ and 10σ starting from 100σ respectively.

FIR3 – A strong bipolar outflow can be seen along NE-SW direction, with red and blue lobes overlapping each other as shown in Figure 3. This tells us that the outflow axis is almost parallel to the line of sight. Red and blue contour intervals are 20σ starting from 40σ and 20σ starting from 60σ respectively.

FIR6b – The contour is not so clear because of other IR sources nearby as shown in Figure 4. The outflow is along the NW-SE direction. Red and blue contour intervals are 10σ starting from 45σ and 10σ starting from 110σ respectively.

MMS2 – The contour is in a tricky situation, because both red and blue lobes are on the east side of the protostar as shown in Figure 5. The outflow structure on the SW side is the outflow from another protostar, MMS5. It is possible that the outflow structure changed shape because of the turbulence from other protostars. Red and blue contour intervals are 10σ starting from 30σ and 10σ starting from 60σ respectively.

MMS5 – There is an outflow structure along the E-W direction as shown in Figure 6. This outflow is much smaller than other bipolar outflows. Red and blue contour intervals are 10σ starting from 20σ and 10σ starting from 40σ respectively.

MMS9 – There is a strong outflow along the E-W direction as shown in Figure 7. We can see a smaller red lobe near the center of the blue lobe. Red and blue contour intervals are 10σ starting from 50σ and 10σ starting from 60σ respectively.

III.1.2 ^{12}CO J = 1 - 0 Observations

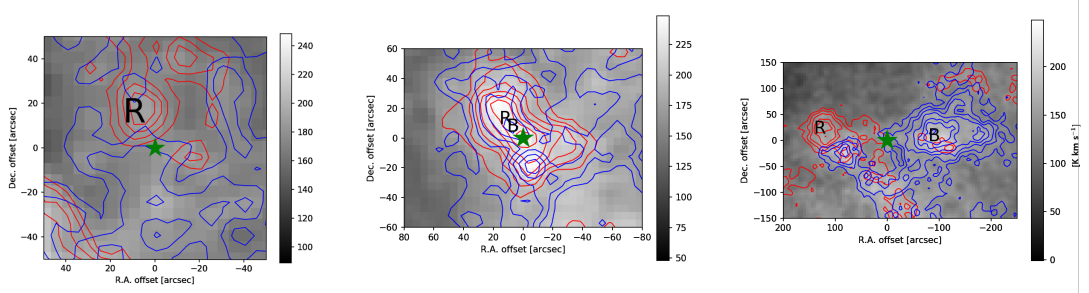


Figure 8. The ^{12}CO J = 1 - 0 intensity contour map of FIR2 (left), FIR3 (middle), and MMS9 (right).

FIR2 – The red lobe is clear on the NW side of the protostar, but the blue lobe is not as clear as shown in Figure 8.

FIR3 – The outflows are in a similar shape as the J = 2 - 1 observations as shown in Figure 8. The lobe centers are slightly near the protostar.

MMS9 – The outflows are also in a similar shape as the J = 2 - 1 observations as shown in Figure 8. We can also see that there is a small red lobe near the center of the blue lobe.

III.2 Momentum Flux

Table 2. CO outflow parameters.

Name	J = 2 - 1			J = 1 - 0		
	F_R	F_B	F_{CO} ($M_\odot \text{ km s}^{-1} \text{ yr}^{-1}$)	F_R	F_B	F_{CO}
FIR2	1.14E-05	3.28E-05	4.42E-05	4.78E-06	-	4.78E-06
FIR3	4.77E-04	7.43E-04	1.22E-03	1.86E-04	3.02E-04	4.88E-04
FIR6b	1.13E-05	1.18E-05	2.31E-05	-	-	-
MMS2	1.14E-05	4.50E-05	5.64E-05	-	-	-
MMS5	5.80E-06	1.55E-05	2.13E-05	-	-	-
MMS9	3.67E-06	1.09E-05	1.46E-05	1.45E-06	6.02E-06	7.47E-06

Table 2 shows the parameters of the outflows detected. F_R and F_B stands for the outflow forces for the red lobe and the blue lobe respectively. F_{CO} is calculated by adding the two forces, which shows the momentum flux of the protostar. We can see that more outflows were detected by using J = 2 - 1 data, and the momentum flux is 2-3 times higher.

III.3 Momentum flux vs. Bolometric luminosity

Figure 9 shows the relation between the bolometric luminosity and the momentum flux of the outflows from previous studies and this work [?, ?, ?, ?, ?, ?]. Since the momentum flux of the same protostar is known to vary somewhat depending on the calculation methods [?], the relation between the bolometric luminosity and the momentum flux is difficult to express with an exact formula and only the degree of tendency can be analyzed.

Orion A Cloud is a region where stars with medium mass are formed. The fact that the momentum flux of the outflow is proportional to the bolometric luminosity can be confirmed.

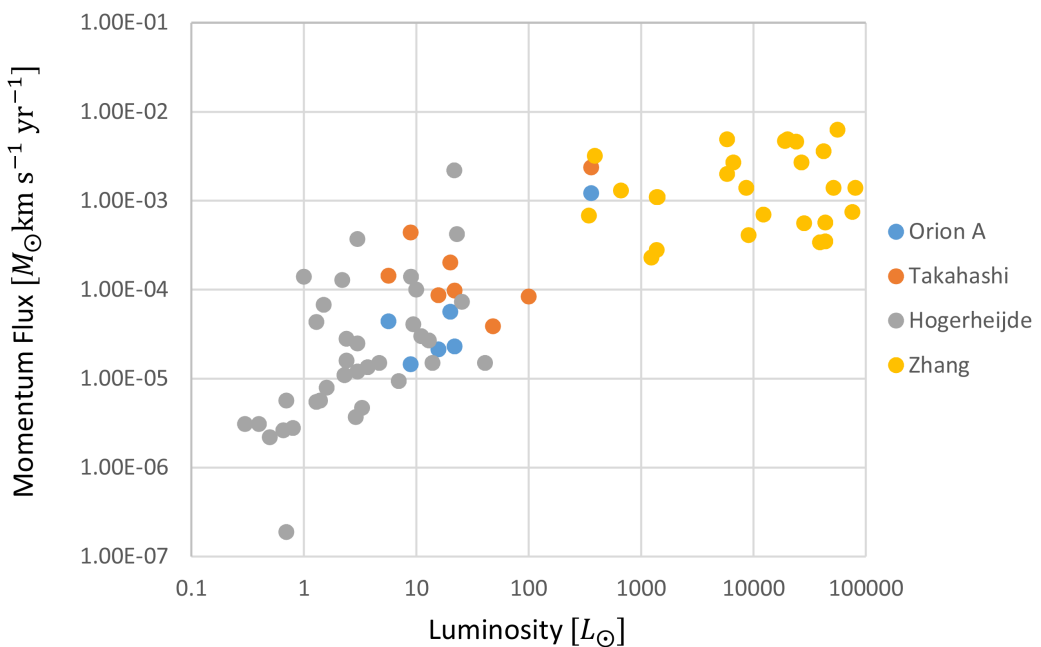


Figure 9. CO outflow momentum flux vs. L_{bol}

III.4 Momentum flux by emission line energy level

Figure 10 compares momentum flux calculated by three different emission lines of the same protostar. The ^{12}CO $J = 3 - 2$ observation was made by Takahashi et al [?]. We can see that it is possible to detect more outflows by using a higher energy emission line of ^{12}CO . Using data with smaller beamwidth also enhances detecting outflows.

The reason that higher energy lines can detect more outflows can be explained as the following: The excitation temperature is higher for emission lines with higher energy. Outflows drag out matter from the protostar's envelope, which has higher temperature than its surroundings. Lines with higher energy are emitted, which has an effect that makes column density higher than usual.

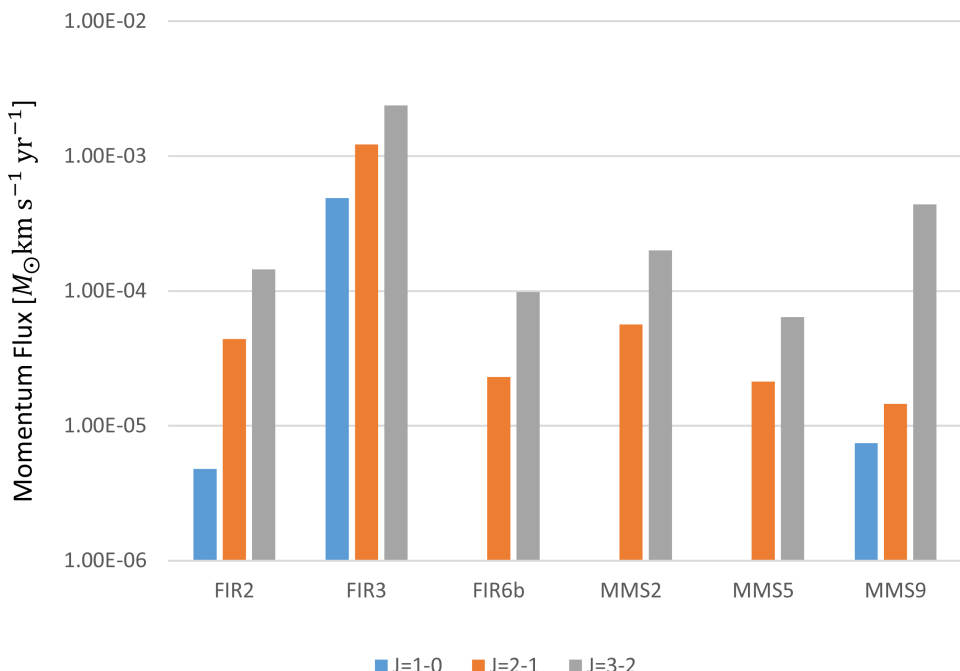


Figure 10. Momentum flux difference by emission line energy.

IV. Conclusion

The main results of this study are as follows:

1. 6 bipolar outflows were detected from the Orion A Cloud. All outflows were detected by $J = 2 - 1$ data and 3 outflows were detected by $J = 1 - 0$ data.
2. The well-known correlation between the momentum flux and the bolometric luminosity can be confirmed.
3. It is possible to detect more outflows by using a higher energy emission line of ^{12}CO . Using data with smaller beamwidth also enhances detecting outflows. The reason that higher energy lines can detect more outflows can be explained as the following. The excitation temperature is higher for emission lines with higher energy. Outflows drag out matter from the protostar's envelope, which has higher temperature than its surroundings. Lines with higher energy are emitted, which has an effect that makes column density higher than usual.

연 구 활 동

- 2017학년도 교내 R&E 발표대회에서 우수상 수상